Electronic Supplementary Material (ESI) for Soft Matter.

Supplementary Information

Effect of Shape Transformations on the Self-Assembly of Faceted Patchy Nanoplates with Irregular Shape into Tiling Patterns

Jaime A. Millan[a], *Daniel Ortiz*[b], *Sharon C. Glotzer**[a,b]

[a]Department of Materials Science and Engineering, University of Michigan, Ann Arbor, MI 48109, USA

[b]Department of Chemical Engineering, University of Michigan, Ann Arbor, MI 48109, USA

*To whom correspondence should be addressed. E-mails: sglotzer@umich.edu

I. Shape Transformations Regular polygons undergo three types of transformations:

Pinching: This transformation can be described as a continuous translation of a single vertex *i* of a regular polygon towards or away from the center of the particle (*O*) (See Fig. S2a). Using the intercep between the radial axis (line that goes through the particle center *O* and vertex *i*) and a perpendicular line segment connecting the nearest vertices *i-1* and *i+1* ias a new reference O' (See left panel in Fig.S2a), the new position of the vertex *i* can be defined by the vector $\vec{a_i}$:

$$\vec{a_i} = 2 * \xi * l_o * \widehat{a_0},$$

where $\widehat{a_0}$ is the unit vector pointing along the radial direction and away from the center of the polygon, l_o is the initial distance from vertex *i* to reference *O'* and ξ is the pinching parameter defined ranging from 0 to 1. For $\xi = 0$ the vertex *i* coincides with O'(left panel in Fig.S2a), for $\xi = 0.5$ the regular polygon is recovered (mid-panel in Fig. S2a) and for $\xi = 1.0$ the polygon is strongly pinched (right panel in Fig.S2a). Under these constraints particle convexity is always preserved and the maximum displacement towards and away to the particle center by a vertex of a regular polygon is the same.

Elongation: This transformation is achieved by simultaneously and continuously rescaling the size of opposite parallel edges by applying the following $operation$: $l' = 2 * \zeta * l_o$, ζ is the final length of the two edges, l_o is the initial edge length of the regular polygon and l' is the elongation truncation parameter ranging 0 to 1(See Fig. S2b). Left, mid-, right panels in Fig. S2b show the case when $l' = 0$ $(\zeta = 0)$, $l' = l_o$ $(\zeta = 0.5$, regular polygon), and $l' = 2 * l_o$ $(\zeta = 1.0)$, respectively. We only apply this transformation on polygons with even number of edges.

Truncation: This transformation is applied on all vertices of the polygon and consists in splitting a vertex of a polygon into a new pair of vertices that lie on the neighboring edges of the split vertex (in Fig. S2c). This transformation doubles the number of edges of polygon. If the initial position of a vertex i is considered as a coordinate reference, and $\widehat{a_1}$, $\widehat{a_2}$ are unit vectors pointing from vertex i to the two closest vertices *i+1* and *i-1* (See leftmost panel in Fig. S2c), then this splitting is accomplished by creating a new pair of vertices represented by vectors $\overrightarrow{v_1}$ and $\overrightarrow{v_2}$ that can be defined as follows (See mid-panel Fig. 21c):

$$\overrightarrow{v_1} = \gamma * l_o{}' * \widehat{a_1}$$
$$\overrightarrow{v_2} = \gamma * l_o{}' * \widehat{a_{2,}}$$

where $l_o{}'$ corresponds to the special case when all edges share the same length after truncation (See right panel in FigS2C) and γ the truncation parameter, respectively. $l_o{}'$ can easily be derived by analyzing the special case when all edges share a similar length (γ = 1) after truncation is applied, leading to the following set of equations (See right panel in Fig. S1c):

$$l_o' = l_o - |\overrightarrow{v_1}| - |\overrightarrow{v'_2}|$$

and,

$$l_o' = \left|\overrightarrow{v'_2} - \overrightarrow{v'_1}\right|,$$

where is initial edge length of the polygon before being truncated. From these equations we arrive to:

$$l'_o = \frac{l_o}{|\overrightarrow{v_2} - \overrightarrow{v_1}| + 2} \quad ,$$

where we have taken into account that $|\overrightarrow{v_1}| = |\overrightarrow{v_2}| = |\overrightarrow{v'_1}| = |\overrightarrow{v'_2}|$.

II. Methods

Monte Carlo Simulation Particles are represented by exact polygonal shapes. Overlap checks are performed as in Ref. (1). In addition to hard-core repulsion, particles interact via a short-ranged potential as explain in the Model and Method section in the main text. Simulation times are several tens of millions of Monte Carlo cycles using established simulation codes.[1,2] System sizes range from 600 to 1000 particles. Self-assembly simulations in the NVT ensemble are performed at constant packing fraction ranging between 0.5 and 0.7 and the temperature is slowly reduced until crystallization is observed. Simulations performed in the NPT ensemble were performed at constant pressure while the temperature is slowly reduced until the system is completely frozen.

II. References

(1) Damasceno, P. F.; Engel, M.; Glotzer, S. C. *Science,* 2012, **337**, 453–457.

(2) Ye, X.; Chen, J.; Engel, M.; Millan, J. a.; Li, W.; Qi, L.; Xing, G.; Collins, J. E.; Kagan, C. R.; Li, J.; Glotzer, S. C.; Murray, C. B. *Nature Chem.* 2013, **5**, 466–473.

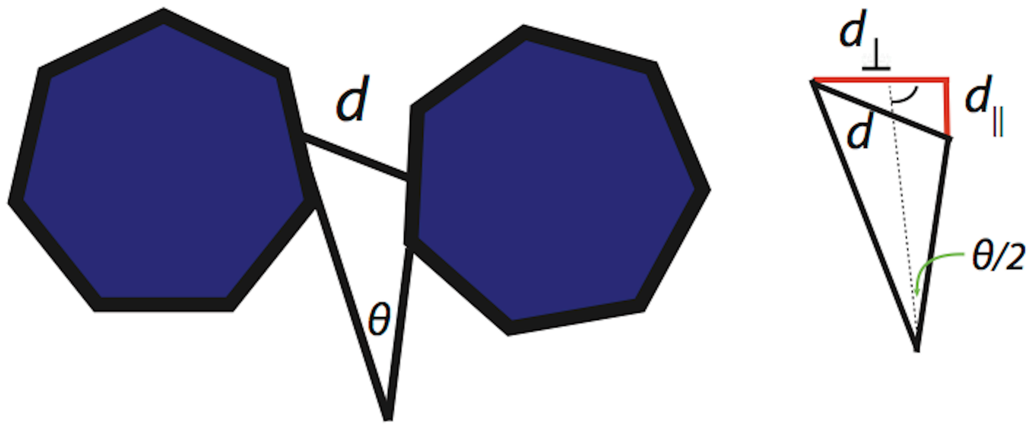

Fig. S1. Interaction model for polygons (nanoplates) and an example of the pinch transformation. a) The interactions between the nanoplates is edge-to-edge and scales linearly with $d_{\perp}$, quadratically with $d_{\parallel}$ and quadratically with orientation angle θ as defined in the Model and Method section.

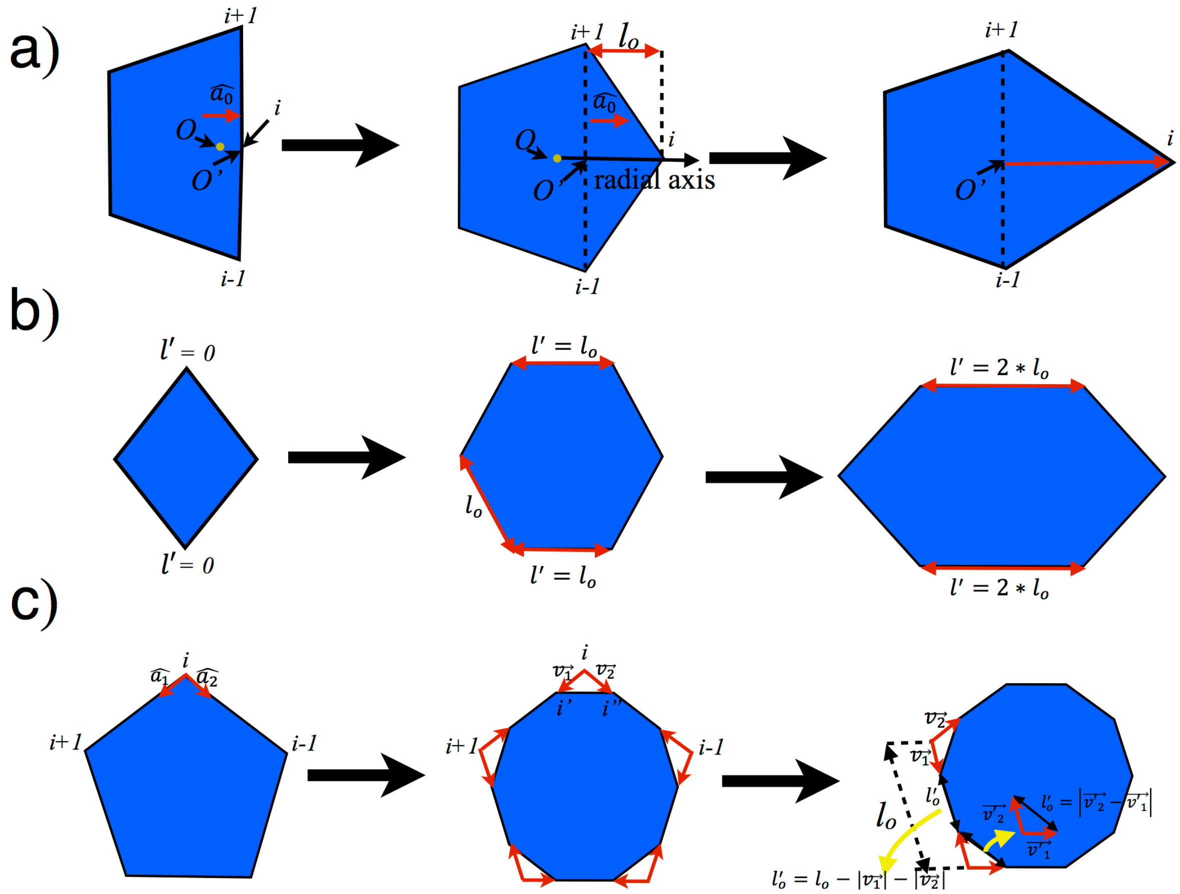

Fig. S2. Schematics of the pinching, truncation and elongation shape transformation. (a) Pinching modifies the shape of a regular polygon continuously by translating a single vertex inwardly or outwardly along the radial direction (axis connecting vertex *i* and particle center *O*. Vertices *i, i+1 i-1,* references *O* and *O'*, radial axis are shown. Left, middle and right panels correspond to $\xi = 0, 0.5$ and 1.0, respectively. (b) Elongation is achieved by rescaling the length (*l'*) of opposite parallel edges (red arrows) with initial length l_o. Left, middle and right panel correspond to the cases when $\zeta = 0$, 0.5 and 1. (c) Left panel shows vertex i and unitary vectors $\widehat{a_1}$ and $\widehat{a_2}$ along which vertex i splits. Vertex i splits into vertices *i'* and *i''* re presented by $\overrightarrow{v_1}$ and $\overrightarrow{v_2}$, and the same operation is applied to each vertex. Left, middle and right panels correspond to γ = 0, 0.5 and 1, respectively. For γ = 1 (right panel), edges share same length $l_o' = \left|\overrightarrow{v'_2} - \overrightarrow{v'_1}\right| = l_o - |\overrightarrow{v_1}| - |\overrightarrow{v_2}|$.

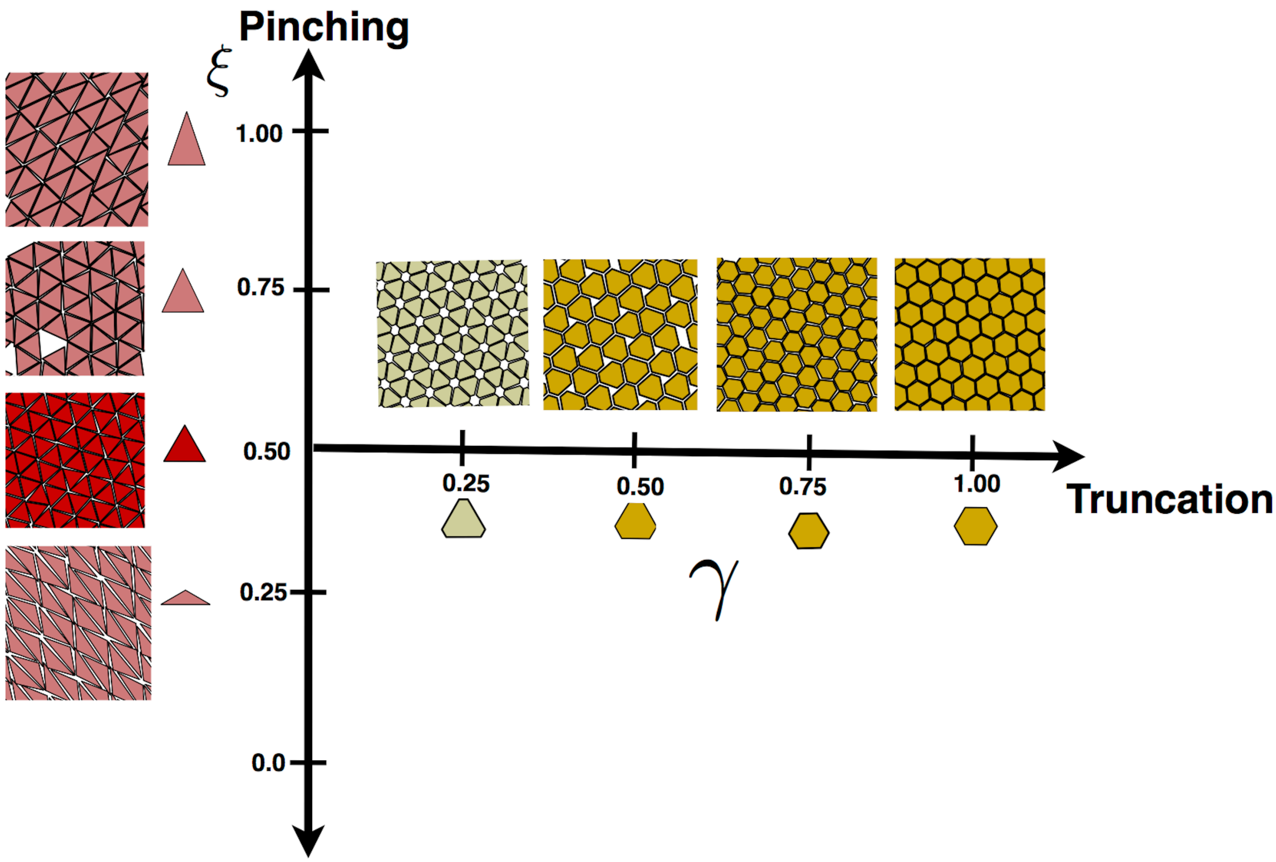

Fig. S3. Phase behavior of triangles along the pinching (ξ) and truncation (γ) shape transformations. Pinching a regular triangle leads towards a transformation from (3^3) Archimedean tilings (ξ = 0.25) to rhombic tilings (ξ = 0.25 and ξ = 0.75 and 1.0). Truncated triangles stabilize porous triangular tilings (γ= 0.25), degenerate ($\gamma \geq 0.25$) and non-degenerate (γ = 0.75 and 1.00) hexagonal (6^6) Archimedean tilings.

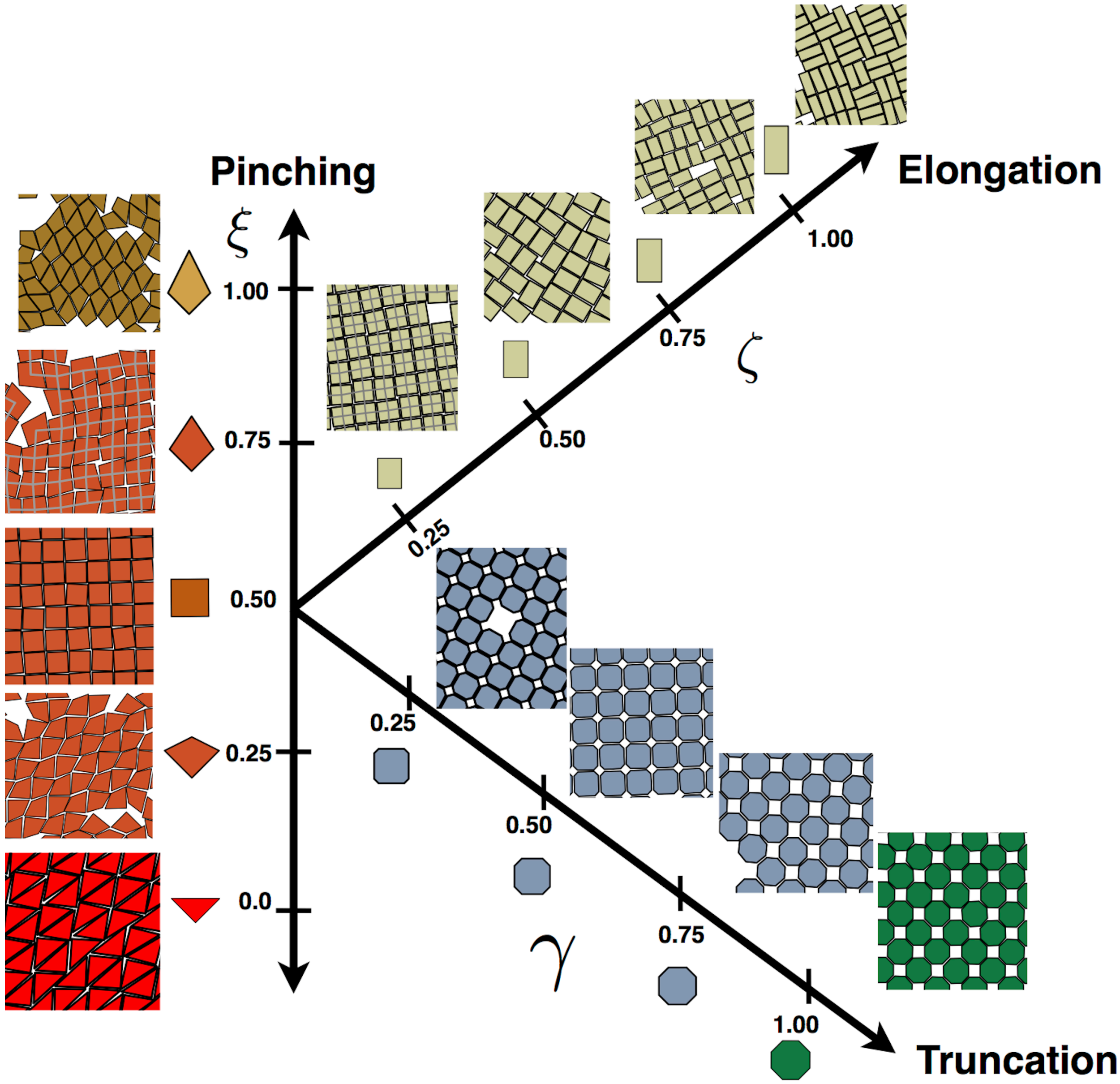

Fig. S4. Phase behavior of squares along the pinching (ξ), truncation (γ) and elongation (ζ) shape transformations. Pinching transforms a squares into a kite leading to the formation of hierarchical kite crystal (ξ = 0.25), square (degenerate) Archimedean tilings (ξ = 0.5 and 0.5) and alternating hierarchical tilings (ξ = 0.75 and 1). Truncation of regular squares leads to the formation of porous squares lattices ($\gamma = 0.25, 0.5$ and 0.75) and ($4^2.8^2$) Archimedean tilings ($\gamma = 1.0$). Slight elongation of regular squares leads to the formation of degenerate squares ($\zeta = 0.25$) and of disorder lattices for $\zeta > 0.25$.

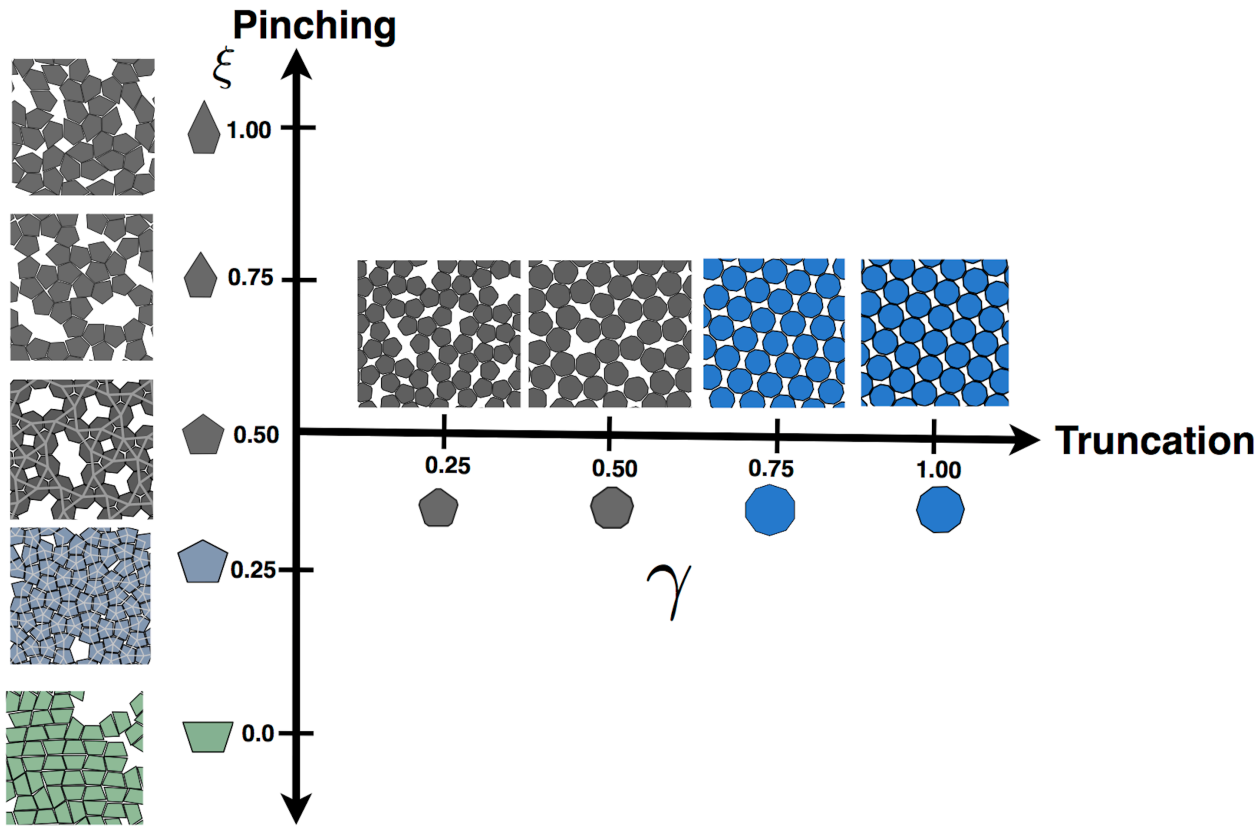

Fig. S5. Phase behavior of pentagons along the pinching (ξ) and truncation (γ) shape transformations. Pinching leads to the formation of trapezoidal tilings (ξ = 0.00), Cairo tilings (ξ = 0.25), frustrated (ξ = 0.50) and disorder assemblies (ξ = 0.75 and 1.0). Slight truncation of pentagons leads to disorder phases. For higher truncation values (γ = 0.75 and 1.0) pentagons behave like decagons and form oblique structures.

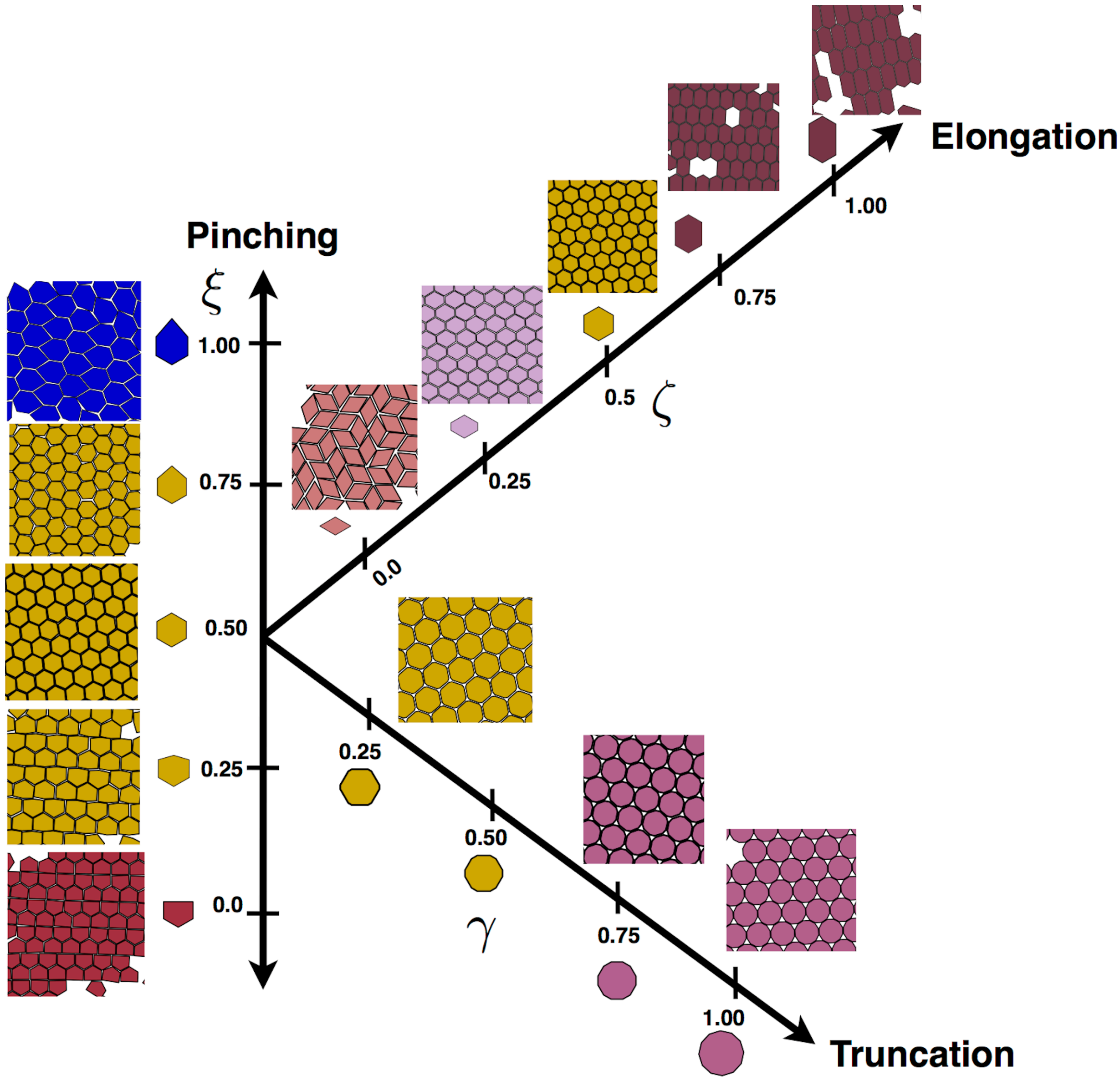

Fig. S6. Pinched hexagons form a prismatic structure ($\xi = 0.00$ and $\xi = 0.25$), a non-degenerate ($\xi = 0.50$) and a degenerate ($\xi = 0.75$) hexagonal (6^6) Archimedean tiling, and an alternating triangular tiling. Truncation of hexagons introduces pores or "empty tilings" to the hexagonal structure. Elongation of hexagons leads to ($\zeta = 0.0$) random tilings, ($\zeta = 0.25$) compressed and elongated ($\zeta = 0.75$ and 1.0) hexagonal (6^6) Archimedean tilings.

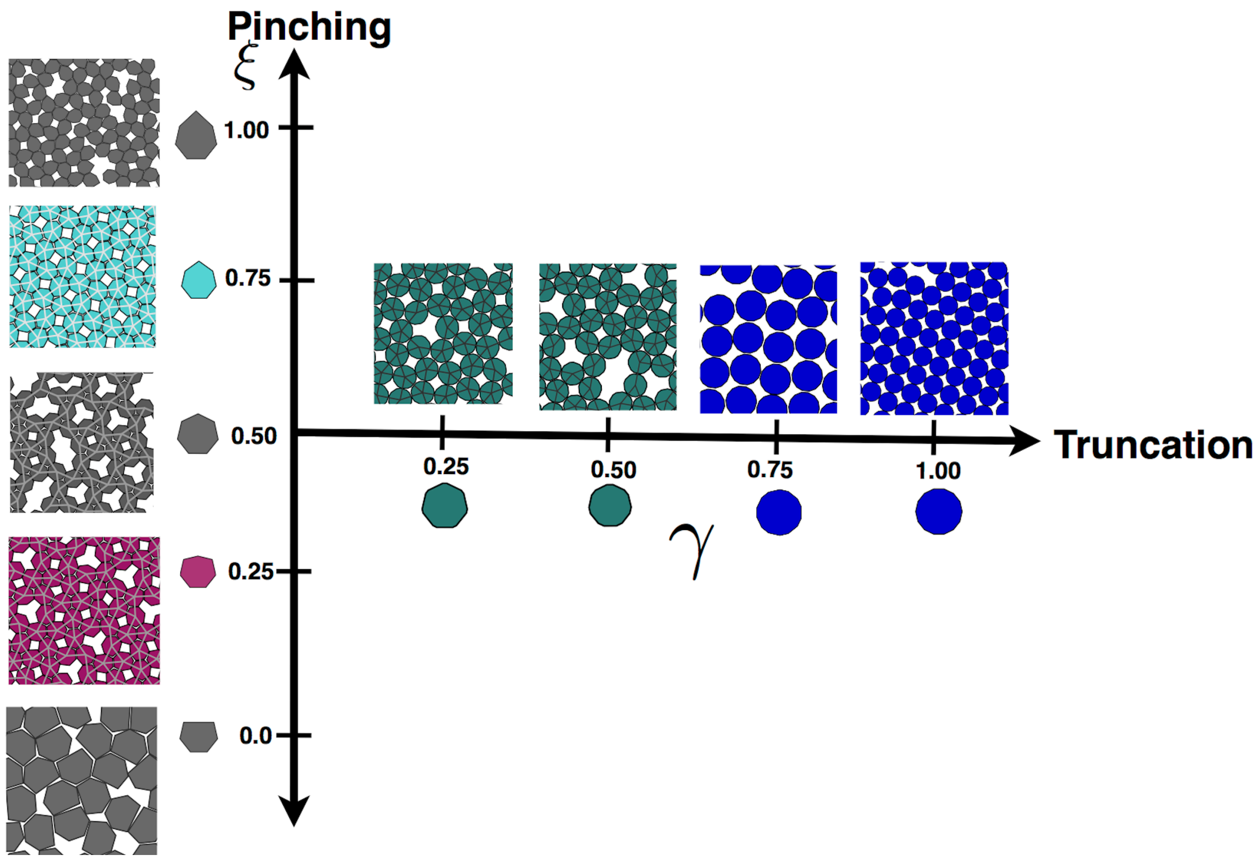

Fig. S7. Phase behavior of heptagons along the pinching (ξ) and truncation (γ) shape transformations. Pinched heptagons self-assemble into a disorder structure (ξ = 0.0), a dodecagonal quasicrystal (ξ = 0.25), a frustrated structure (ξ = 0.5), an (3^2.4.3.4) Archimedean tiling (ξ = 0.75) and a frustrated structure (ξ = 1.0). Truncated heptagons stabilize dodecagonal quasicrystals (γ = 0.25 and 0.5) and center rectangular tilings ($\gamma \geq 0.75$).

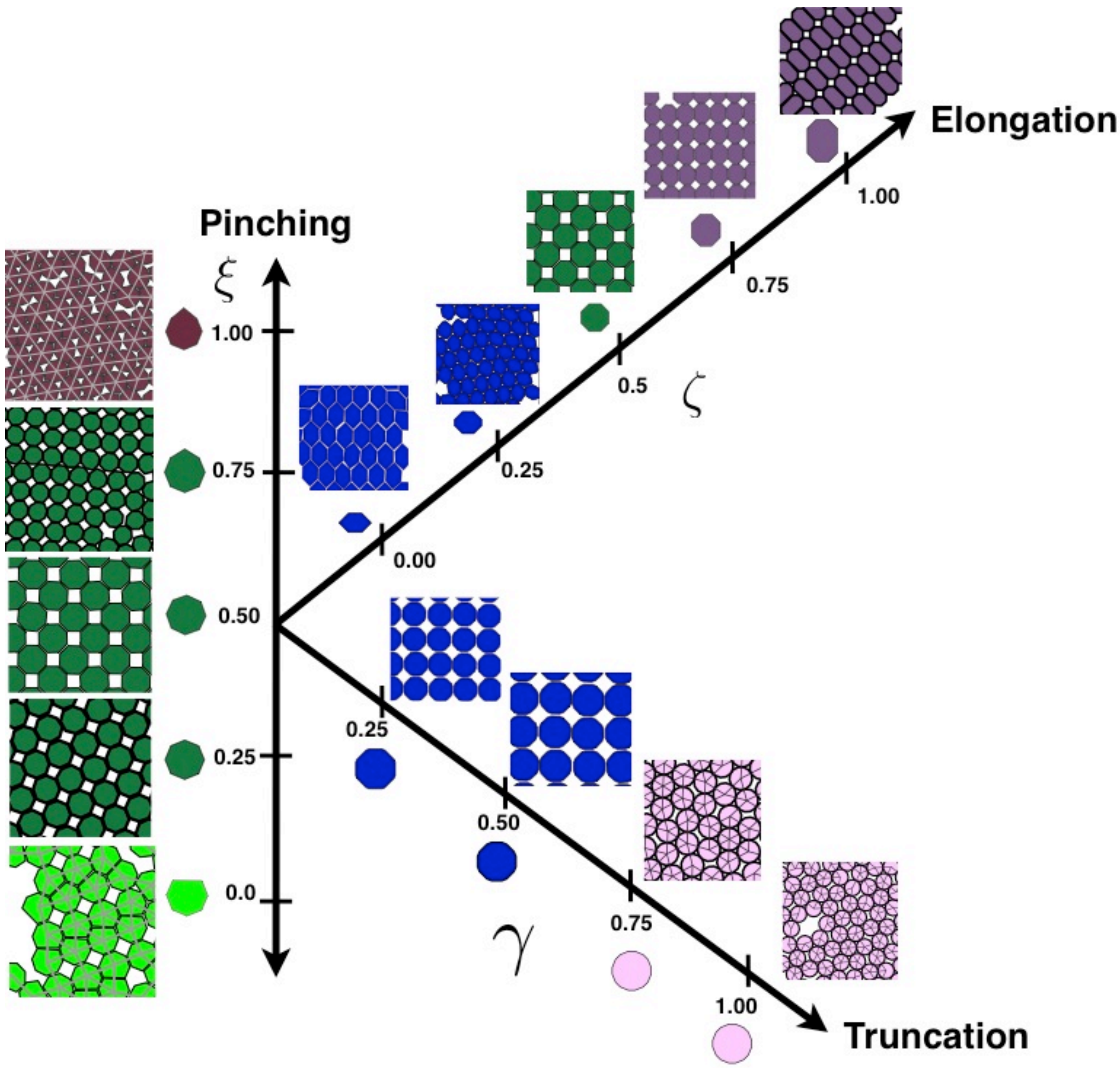

Fig. S8. Phase behavior of octagons along the pinching (ξ), truncation (γ) and elongation (ζ) shape transforms. The following structures are for the observed for the pinching transformation: ($3^3.4^2$) Archimedean tilings (ξ = 0.00), a (4.8^2) Archimedean tilings (ξ = 0.25, 0.5) which is degenerate for ξ = 0.75, and degenerate triangular tilings (ξ = 1.00). Truncation of regular octagons transform Archimedean tilings into star polygon tilings for $\gamma = 0.25$ and 0.5. Further truncations lead to disk behavior. Elongation leads to parallel arrangements ($\zeta = 0.0$), shortened ($8^2.4$) Archimedean tilings ($\zeta = 0.25$), ($8^2.4$) Archimedean tilings ($\zeta = 0.5$), and elongated ($8^2.4$) Archimedean tilings $\zeta =$ 0.75 and 1.0.

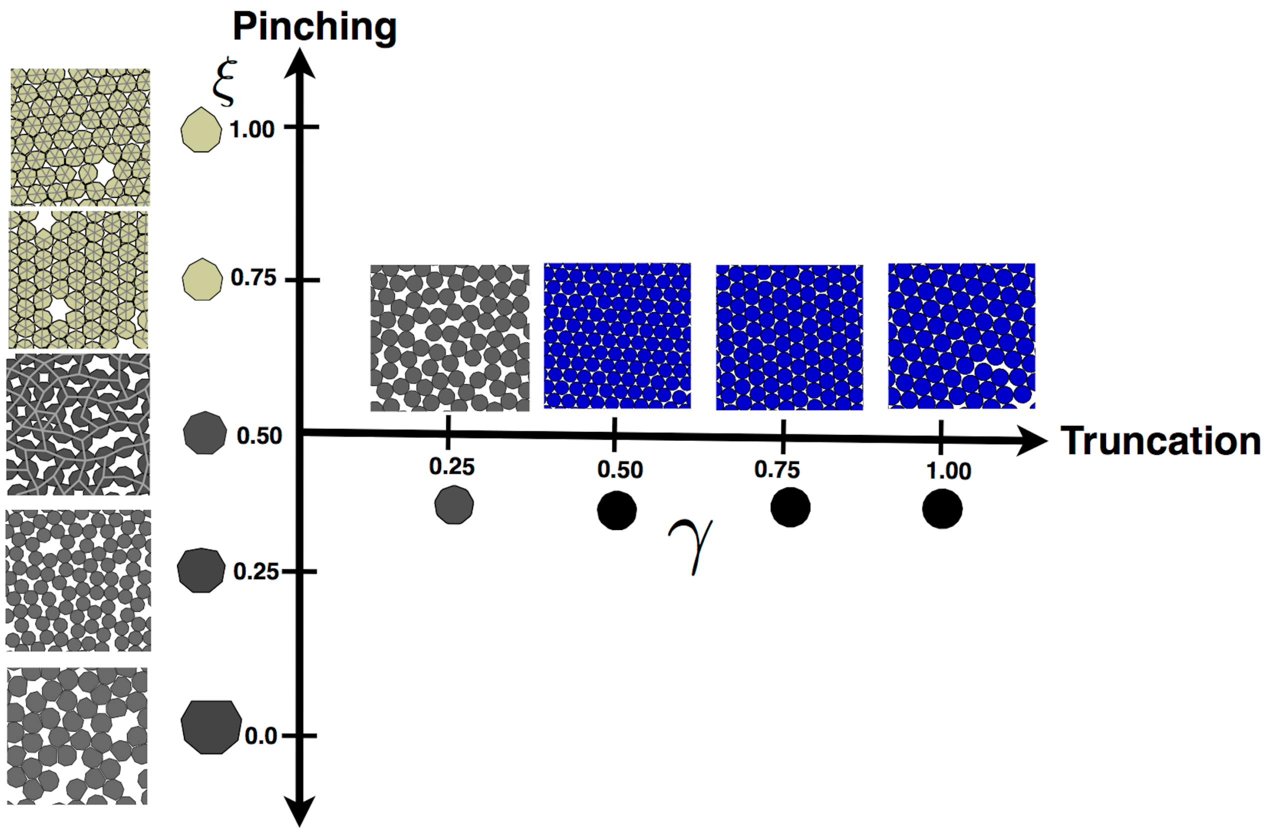

Fig. S9. Phase behavior of nonagons along the shape pinching (ξ) and truncation (γ) shape transformations. Pinching leads to the formation of disorder tilings (ξ = 0.00, 0.25 and 0.5), and degenerate triangular lattice (ξ = 0.75 and 1.0). Slightly truncation leads disorder structures (ξ = 0.25 and 0.5), and further truncations leads to disk behavior were nonagons form hexagonal degenerate tilings (ξ = 0.50, 0.75 and 1.0).

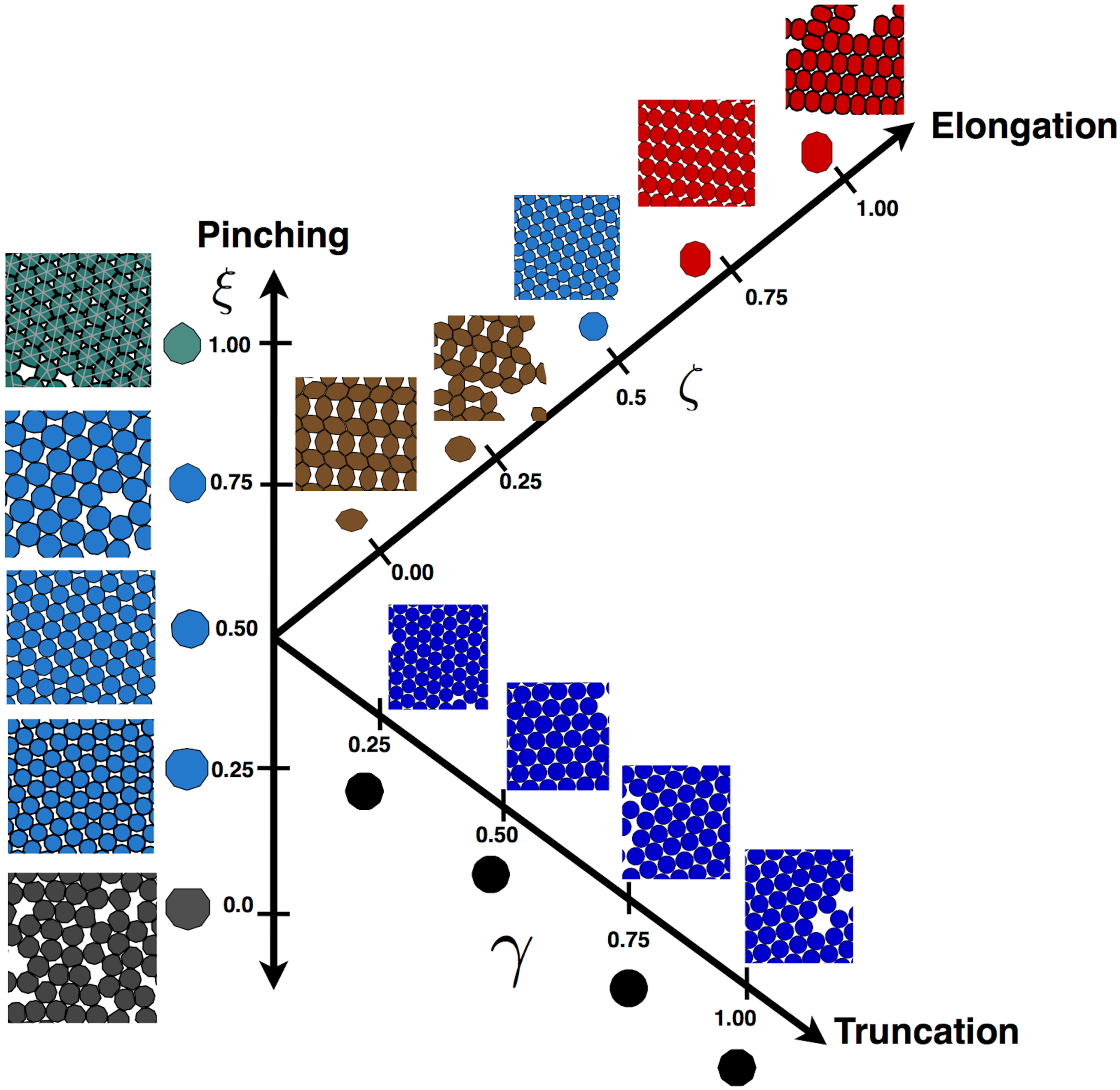

Fig. S10. Phase behavior of decagons along the pinching (ξ), truncation (γ) and elongation (ζ) shape transformations. The following structures are for the observed for the pinching transformation: a disorder tilings (ξ = 0.00), parallel lattices (ξ = 0.25, 0.50, 0.75) and triangular tilings (ξ = 1.00) Truncation (γ) leads to disk behavior. Elongation leads complex porous structures (ζ = 0.25 and 0.5), further elongation (ζ = 0.50, 0.75 and 1.00) leads to (elongated) parallel lattices that resemble structures self-assembled from sticky decagons.

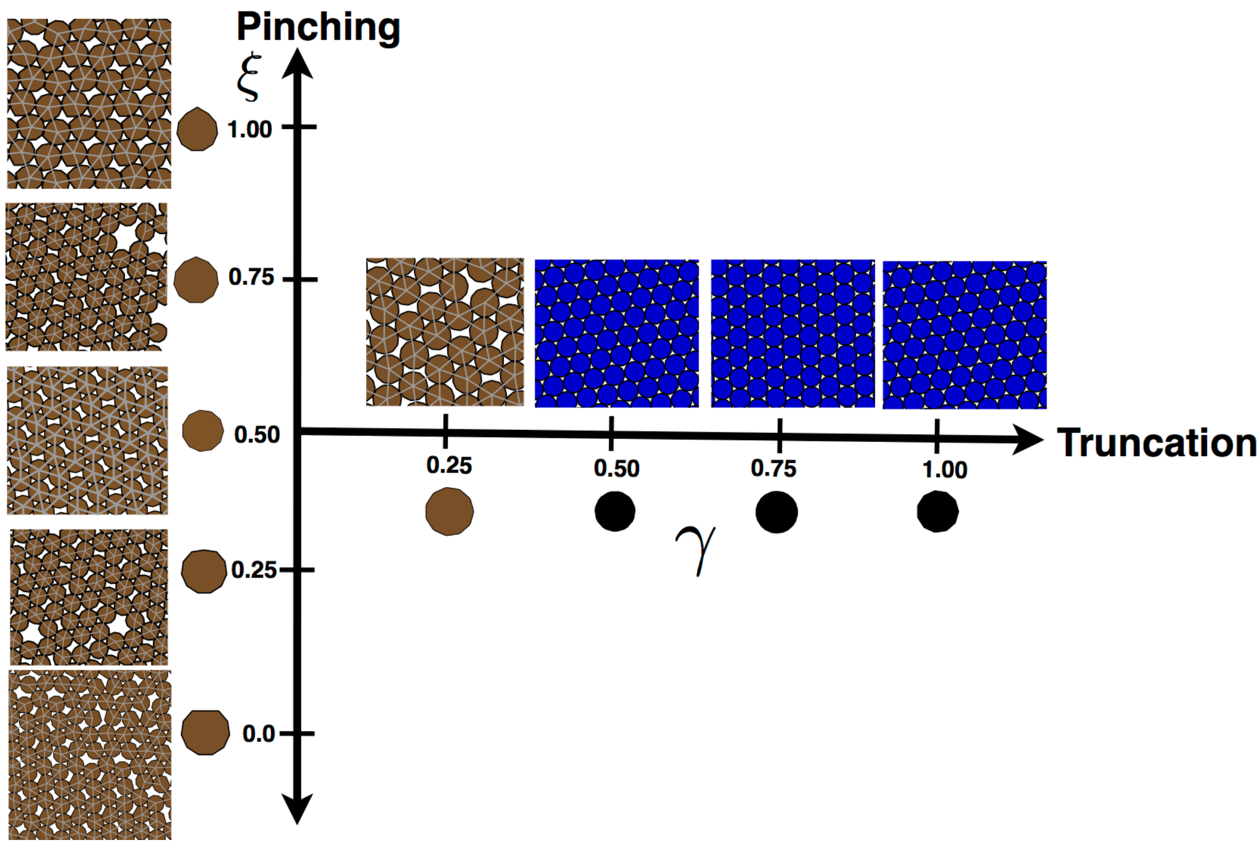

Fig. S9. Phase behavior of hendecagons along the pinching (ξ) and truncation (γ) shape transformations. Regarding of the amount of pinching applied on the nonagons; a sheared (3^2.3.4.3) Archimedean tiling is observed. Slightly truncated nonagons form (3^2.3.4.3) Archimedean tiling (ξ = 0.25), and further truncations leads to disk behavior were nonagons form hexagonal degenerate tilings (ξ = 0.25 and 0.5, 0.75 and 1.0).

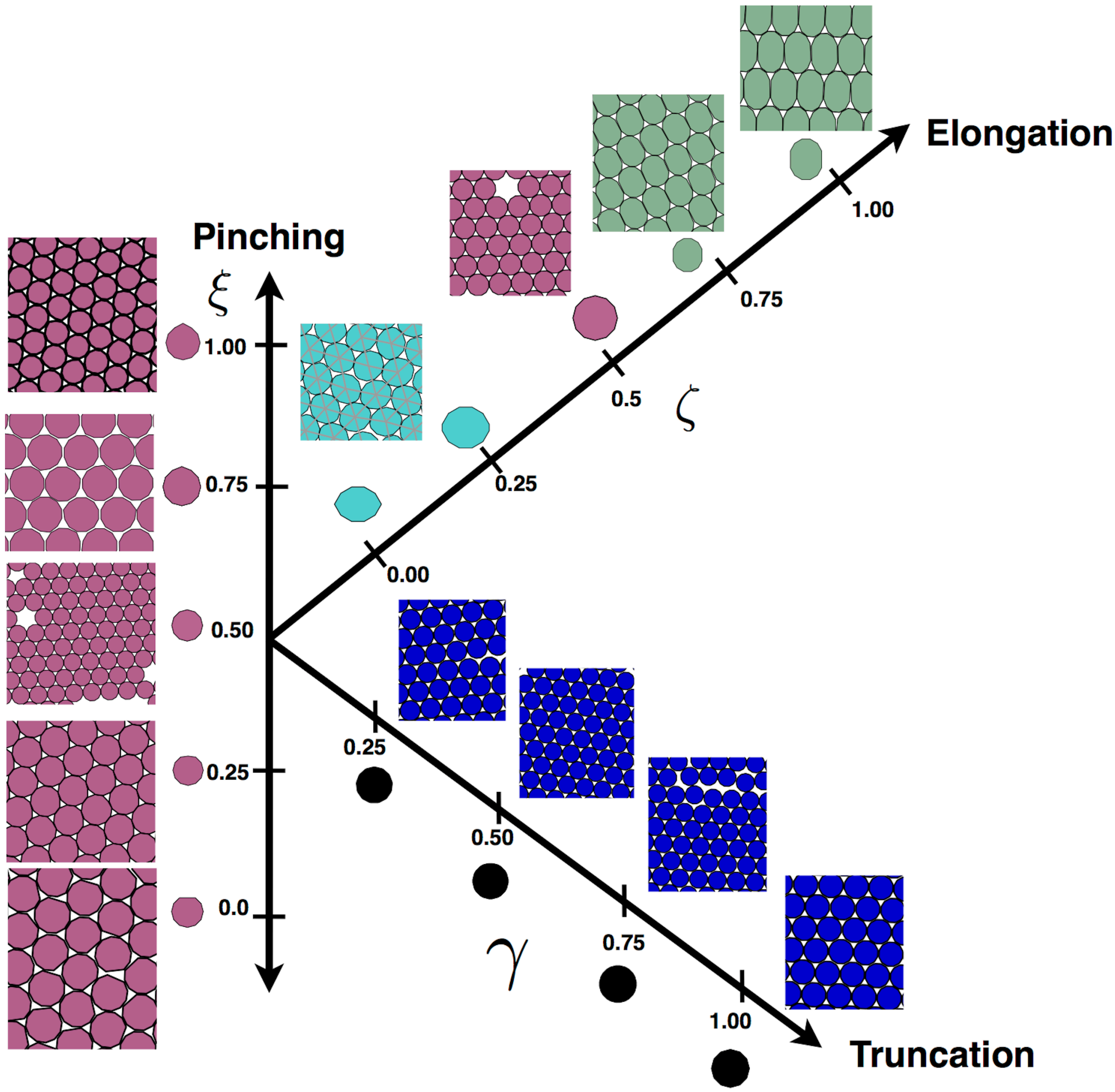

Fig. S10. Phase behavior of dodecagons along the pinching (ξ), truncation (γ) and elongation (ζ) shape transformations. Regardless of pinching applied on the dodecagons, hexagonal center-to-center tilings are observed. For intermediate and high pinching (3.12^3) Archimedean tiling are self-assembled. Truncation (γ) leads to disk behavior. Elongation leads to degenerate triangular lattices for compressed dodecagons ($\zeta = 0.00$ and 0.25), further truncations leads to (elongated) 3.12^3) Archimedean tiling for $\zeta = 0.50$, 0.75 and 1.00.